



# Electrochemical detection of Zika and Dengue infections using a single chip

Isabella Sampaio<sup>\*</sup>, Felipe Domingues Quatroni, Juliana Naomi Yamauti Costa, Valtencir Zucolotto

*GNano – Nanomedicine and Nanotoxicology Group, Physics Institute of São Carlos, University of São Paulo, CP 369, 13560-970, São Carlos, SP, Brazil*

## ARTICLE INFO

### Keywords:

Zika detection  
Dengue detection  
Multiplex device  
Electrochemical biosensor  
SARS-CoV-2  
Simultaneous detection

## ABSTRACT

Zika and Dengue are infectious diseases caused by flaviviruses and transmitted by *Aedes* mosquitoes. Although symptoms are usually mild, complications such as dengue hemorrhagic fever and microcephaly in newborns -after the pregnant woman becomes infected with the Zika virus-have emerged as a global public health concern. The co-circulation of Zika and Dengue viruses and the overlapping of their symptoms represent a challenge for the accurate diagnosis. A single test for the point-of-care detection of both diseases is crucial. Here we report a single chip that distinguishes between Zika and Dengue infections using the non-structural protein 1 (NS1) as biomarkers. A novel multiplex electrochemical device containing four independent working electrodes was developed. Zika and Dengue biosensors were fabricated separately on different working electrodes. Selectivity tests showed that the two biosensors can distinguish not only the NS1 proteins from Zika and Dengue but also the spike proteins present in the SARS-CoV-2. This is especially relevant as patients with COVID-19 may have symptoms similar to Zika and Dengue. The gold surface was modified with cysteamine and antibodies against the NS1 proteins. Both biosensors detected their respective biomarkers at clinically relevant concentrations and presented a good linear relationship between the percentage change in impedance and the logarithm of the NS1 concentration ( $R^2 = 0.990$  for Dengue and  $R^2 = 0.995$  for Zika). Upon combining a simple sample preparation with a portable detection method, our disposable multiplex device offers a point-of-care diagnostic test for Zika and Dengue using a single chip. Additionally, two other biosensors can be added to the chip, providing a platform for viral detection.

## 1. Introduction

Zika and Dengue are infectious diseases caused by flaviviruses and mainly transmitted by *Aedes aegypti* mosquitoes, typically found in tropical and subtropical countries (Brito et al., 2021; Rajah et al., 2016). In the early stages, both diseases have similar symptoms such as fever, nausea, and joint pain (Rajah et al., 2016; Wilder-Smith et al., 2019). According to the World Health Organization, the estimated number of infections caused by the Dengue virus (DENV) per year worldwide is about 390 million. In recent years, an alarming increase in the incidence of this disease has been noted (WHO. Dengue and severe dengue, 2021). Despite the low mortality of the disease, cases of severe Dengue can occur, especially upon secondary infection (Wilder-Smith et al., 2019). In 2015, an outbreak of Zika virus (ZIKV) occurred in Brazil and quickly spread to other countries in America and Africa. An association between ZIKV infection in pregnant women and microcephaly in newborns was identified, making it a global public health concern (Sarkar and Gardner,

2016). The impact on health services caused by the overlapping of Zika and Dengue epidemics in addition to the absence of vaccines and specific treatments show the demand for early diagnosis methods capable of identifying and differentiating them. This is essential to update the epidemiological data, as well as to map the geographic distribution of diseases and to take more effective prevention and control measures (Cecchetto et al., 2020). The main diagnostic methods available for Zika and Dengue are viral isolation, molecular analyses, and serological identification (Yang and Narayan, 2017). The molecular confirmation through reverse transcription-polymerase chain reaction (RT-PCR) is the gold standard method, however, it requires expensive equipment and highly trained employees. Viral isolation requires a couple of days of cell cultures incubation, being not efficient in the clinical setting (Faria and Zucolotto, 2019). Therefore, the serological test by enzyme-linked immunosorbent assay (ELISA), in which IgG and IgM antibodies produced in response to viral infection are screened, is still the simplest and most widely used (Lima et al., 2019). Although these methodologies are

<sup>\*</sup> Corresponding author.

E-mail address: [isbellasampaio@gmail.com](mailto:isbellasampaio@gmail.com) (I. Sampaio).

<https://doi.org/10.1016/j.bios.2022.114630>

Received 8 April 2022; Received in revised form 27 June 2022; Accepted 6 August 2022

Available online 17 August 2022

0956-5663/© 2022 Elsevier B.V. All rights reserved.

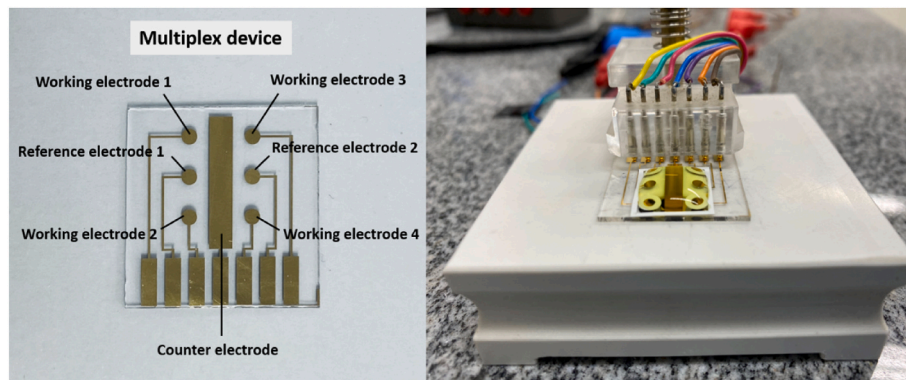


**Fig. 1.** Gold multiplex device containing four working electrodes, two reference electrodes, and one counter electrode (a). Measurement setup: electrolyte solution covering the multiplex device and the connector used to connect the electrodes to the potentiostat (b).

powerful diagnostic tools, multiplex versions for simultaneous detection of Zika and Dengue can be labor-intensive and time-consuming, increasing the assay cost and complexity.

Biosensors represent a great alternative because they can be designed to detect multiple analytes with high specificity and can offer portable and cost-effective platforms. Although they are being widely explored for individual detection of ZIKV and DENV, there are few multiplex biosensors reported for simultaneous testing and involve RNA identification of ZIKV and DENV (Xie et al., 2018; Lee et al., 2020; Priye et al., 2017), which require a more complex sample preparation step, or a high-cost detection technique whose portability is limited (Sánchez-Purrà et al., 2017). To develop a point-of-care test, biosensors that detect antigens or antibodies are preferred. Recent studies have shown that the non-structural protein 1 (NS1) may represent an efficient biomarker to discriminate DENV infection from ZIKV infection, providing limited cross-reactivity due to group-specific epitopes (Lima et al., 2019). NS1 is a glycoprotein continuously secreted by the infected host cells and is found at high concentrations in the blood during the early clinical phase of the disease (Dias et al., 2013; Bachour Junior et al., 2021). Up to 7 days of symptoms, the typical plasma NS1 concentrations are 30 ng/mL for Zika and 120 ng/mL for Dengue (clinical range 0.01–2 µg/mL) (Santos et al., 2018; Bosch et al., 2017).

To address these challenges, we designed a multiplex electrochemical biosensor for the detection of Zika and Dengue infection on a single chip using as target molecules the NS1 proteins from Zika (NS1ZV) and Dengue (NS1DV). The device comprises four working electrodes, being two of them used as the Zika Dengue biosensors. The biorecognition layer was constructed using the self-assembled monolayer technique. The gold surface of the working electrodes was modified with cysteamine and then with antibodies against target proteins. Electrochemical impedance spectroscopy (EIS) technique was used to monitor surface functionalization and analyte detection. The biosensors on the multiplex platform were able to detect their analytes with high specificity, without cross-reactivity between NS1DV, NS1ZV, and spike protein (COVID-19). This portable system is suitable to be applied point-of-care because it offers simple and fast analysis (~10 min). Therefore, the multiplex device reported here can provide a single test for detecting multiple viral diseases, aimed at the early screening of patients, especially in epidemic situations.

## 2. Experimental

### 2.1. Materials

Zika Virus (ZIKV-NS1) Monoclonal Antibody (MBS568046), Zika Virus (ZIKV-NS1) Antigen (MBS568704), COVID-19 Spike Protein (MBS2563881), and Dengue Virus NS1 Type 2 protein (MBS143474) were purchased from Mybiosource (San Diego, CA, USA). Dengue NS1

monoclonal antibody (10–1495) was acquired from Fitzgerald Industries International (Acton, MA, USA). N-Hydroxysuccinimide (NHS), N-(3-Dimethylaminopropyl)-N'-ethylcarbodiimide hydrochloride (EDC), cysteamine, potassium chloride, potassium ferricyanide, potassium ferrocyanide, dibasic sodium phosphate, monobasic sodium phosphate dihydrate, potassium hydroxide, were acquired from Sigma-Aldrich. Acetone and ethanol were purchased from Labsynth (Diadema, SP, Brazil). The phosphate buffer (PBS, 10 mM, pH 7.4), was prepared using 2.1 mM monobasic sodium phosphate dihydrate, 7.9 mM sodium phosphate dibasic, and 0.1 M sodium chloride. Milli-Q purified ultra-pure water (Resistivity = 18.2 MΩ cm) was used to prepare all aqueous solutions.

### 2.2. Fabrication of multiplex devices

A novel multiplex device was developed to enable the electrochemical detection of up to 4 diseases on a single chip. As shown in Fig. 1, the biosensor device has four working electrodes, two reference electrodes, and a counter electrode. The area of the working and reference electrodes is 3.14 mm<sup>2</sup> and the counter electrode is 70 mm (Rajah et al., 2016). To maintain the distance between the electrodes, the reference 1, which is located on the left side, is used to measure the working electrodes on that same side (1 and 2). Similarly, reference electrode 2 is used in the measurements of working electrodes 3 and 4. The multiplex was fabricated by photolithography and sputtering techniques. In the photolithography step, the substrates (BK7 glasses) were modified with photoresist, a photosensitive film, by the spin-coating technique and left on a hot plate at 90 °C for 10 min. Then, they were exposed to ultraviolet light through an optical mask containing the desired device configuration. In this case, a positive photoresist was used and the light-exposed regions were subsequently removed by immersing the substrates in a developing chemical solution (aqueous potassium hydroxide solution). Finally, to remove the organic residues, the substrates were cleaned with oxygen plasma. Metallization was carried out in a vacuum chamber and the thickness of the deposited tracks was measured by a quartz crystal. For better gold adhesion, a 20 nm-thick titanium film was deposited on the substrates, which was further covered with a 120 nm-thick gold layer. The topography of the working electrodes was analyzed by atomic force microscopy (AFM). The images were collected in a Nanosurf Flexa microscope (Nanosurf, Switzerland), in the tapping mode, using a silicon cantilever with a resonance frequency of 190 kHz and a force constant of 48 N/m. Roughness was assessed from 2 µm (Rajah et al., 2016) images with a resolution of 512 pixels by the Gwyddion software.

### 2.3. Electrode modification

The electrodes were cleaned by sonication for 5 min using an

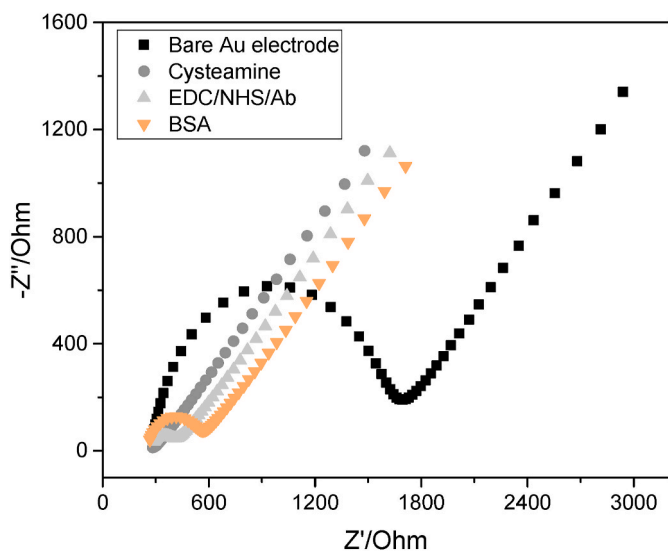


**Fig. 2.** Nyquist diagrams showing the electrode functionalization steps obtained in 0.1 M KCl solution containing 5 mM  $[\text{Fe}(\text{CN})_6]^{3-/4-}$ . Inset: upper: electric equivalent circuit best fitted to the impedance curves. Lower: zoomed area of the Nyquist diagram detailing the impedance evolution for the four analyses.

ultrasound bath in a sequence of solutions (acetone, Milli-Q, 2% KOH in ethanol, ethanol, Milli-Q) and dried in  $\text{N}_2$  flow. The working electrodes were modified by the self-assembled monolayer (SAM) method. First, 5  $\mu\text{l}$  of a 0.5 M cysteamine solution was added to the electrodes and left to incubate for 15 h at 4  $^\circ\text{C}$ . Then, a solution containing EDC, NHS, and the antibody at concentrations of 8 mM, 5 mM, and 40  $\mu\text{g}/\text{mL}$ , respectively, was added to the electrode and left for 3 h at 4  $^\circ\text{C}$ . This solution was previously incubated for 2 h to activate the carboxyl groups of the antibodies through the reaction with EDC/NHS. Finally, the surface was blocked with 1% BSA in PBS for 30 min. Between steps, electrodes were washed by subsequent immersion in 10 mM PBS (pH 7.4) and Milli-Q, and then dried in  $\text{N}_2$  flow.

#### 2.4. Electrochemical measurements

The cyclic voltammetry (CV) and electrochemical impedance spectroscopy (EIS) measurements were performed in a PGSTAT204 potentiostat (Metrohm Autolab) using 0.1 M KCl as electrolyte solution containing 5 mM of the  $[\text{Fe}(\text{CN})_6]^{3-/4-}$  redox couple. For this, 350  $\mu\text{l}$  of electrolyte solution were added to the device surface, covering all electrodes as shown in Fig. 2. The electrodes were first submitted to CV measurements for surface preparation and then to EIS measurements. For CV measurements, 2 cycles were performed in the potential range

from  $-0.5$  to  $0.6$  V at a scan rate of 50 mV/s. EIS analyzes were performed in the frequency range from 10 kHz to 0.1 Hz with AC amplitude of 10 mV at open circuit potential. The equivalent circuit and the charge transfer resistance ( $R_{\text{CT}}$ ) were determined using NOVA 2.1 software. For the detection tests, 5  $\mu\text{l}$  of the samples were added to each working electrode, with the area delimited by an inert adhesive. The samples were incubated for 30 min and washed by immersion in PBS. The measurement of each working electrode takes about 2.5 min. The entire chip is measured within 10 min.

### 3. Results

#### 3.1. Electrode characterization and functionalization

The electrode roughness is an important parameter, that may influence the biosensor performance. Studies show that electrochemical measurements performed on rougher electrodes are less reproducible, as their surface favors the formation of defects in the monolayer (Butterworth et al., 2019; Dutta et al., 2021). AFM images collected after cleaning the working electrode (Fig. S1, Supporting information) show a highly smooth surface compared to commercial disposable gold electrodes (Butterworth et al., 2019). The maximum height obtained was 29 nm and the mean square roughness ( $R_q$ ) was 1.22 nm. The smooth profile of these electrodes can be attributed to the thickness of the deposited gold layer and the chosen substrate. Therefore, these results demonstrate that the fabricated multiplex devices have electrodes with an ideal topographic profile for the development of reproducible electrochemical biosensors.

Surface modification was evaluated by the EIS technique. After each step, the electrodes were subjected to impedance measurements. The equivalent circuit that presented the best fit to the spectra was the Randles model, which was used to determine the  $R_{\text{ct}}$  of the electrodes. As shown in Fig. 2, after incubation with the cysteamine solution, the electrode impedance is drastically decreased and the semicircle is barely formed. This behavior can be attributed to the positively charged amine groups of cysteamine, which attract anions from the electrolytic solution used in the measurement. The latter demonstrates the efficient functionalization of the electrode surface with cysteamine molecules through the thiol-gold bond. After the incubation with antibodies and blocking with BSA steps, an increase in impedance is observed, indicating that these biomolecules were immobilized on the electrode surface. At this point, it is worth noting that the cysteamine concentration is quite high, for this reason, even with the immobilization of antibodies and BSA, the impedance remains lower than that presented by the bare electrode.

#### 3.2. Detection and cross-reactivity tests

Biosensors for Dengue and Zika diagnosis were fabricated separately

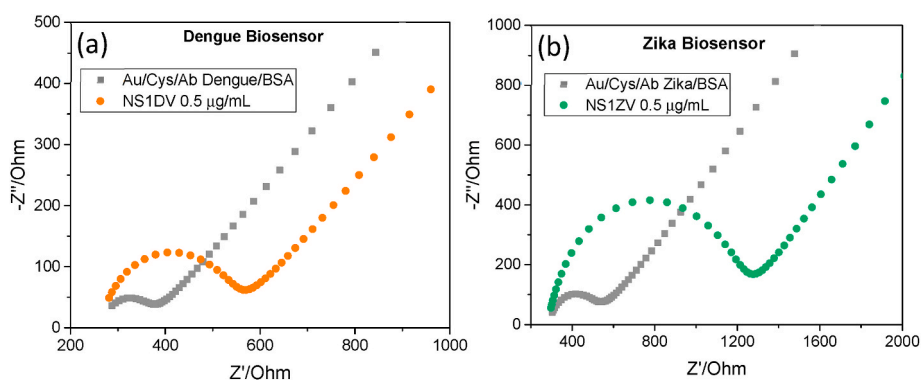


**Fig. 3.** Nyquist diagrams of Dengue (a) and Zika (b) biosensors fabricated on the multiplex device before and after incubation with target proteins.

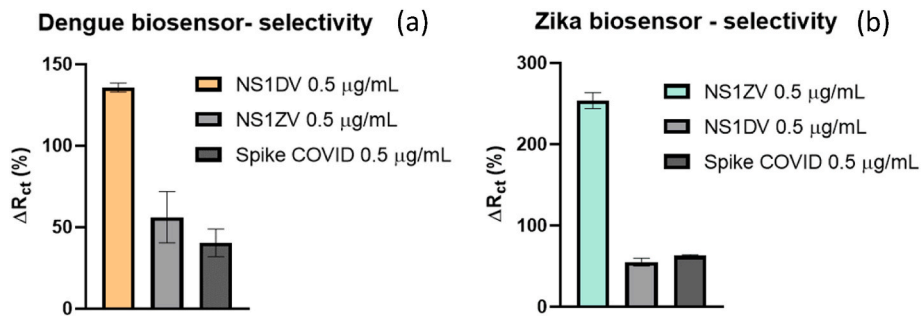


**Fig. 4.** Selectivity tests of Dengue (a) and Zika (b) biosensors. Bars show the percent change in  $R_{ct}$  after incubation with target and negative proteins. For the Dengue biosensor, the NS1ZV and the spike protein of SARS-CoV 2 (COVID-19) were tested. For the Zika biosensor, the chosen negative proteins were NS1DV and Spike. All tests were performed in triplicate ( $n = 3$ ).

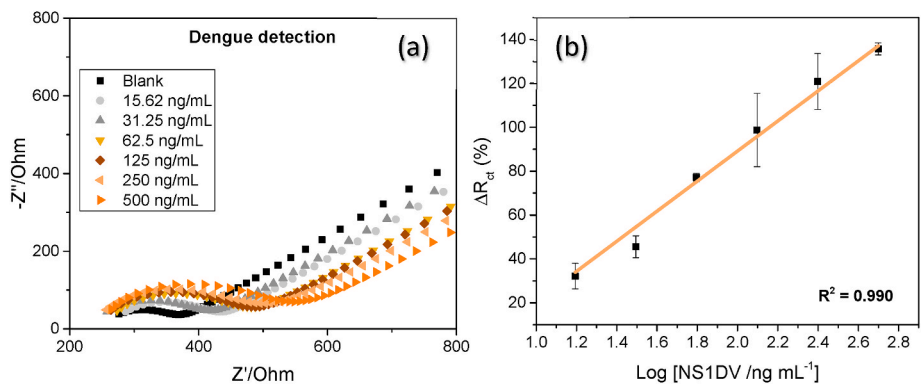


**Fig. 5.** Analytical curve of the Dengue biosensor in the range of 15.62–500 ng/mL. The Nyquist plots (a) and the linear fit (b) show a linear relationship between the percent change in  $R_{ct}$  and the logarithm of the NS1DV concentration. Each concentration was tested on 3 independent electrodes ( $n = 3$ ).

using anti-NS1DV and anti-NS1ZV antibodies, respectively. After incubation with their target proteins at 0.5  $\mu\text{g/mL}$  for 30 min, electrochemical measurements were performed and the percentage change in  $R_{ct}$  was calculated as  $\Delta R_{ct} (\%) = 100 \times [R_{ct} \text{ after} - R_{ct} \text{ before} / R_{ct} \text{ before}]$ . An increase in  $R_{ct}$  of 137% was obtained for the Dengue biosensor and 254% was obtained for the Zika biosensor (Fig. 3), demonstrating that both were able to detect their analytes.

In order to assess the ability of the biosensor to correctly differentiate the target protein from proteins that are biomarkers of other diseases, whose initial symptoms are very similar, we conducted the cross-reactivity tests. NS1ZV and Spike protein-a biomarker of the SARS CoV-2 virus that causes COVID-19 - were used as negative controls for the Dengue biosensor. As shown in Fig. 4a, the incubation with the NS1ZV protein increased the  $R_{ct}$  by  $56 \pm 16\%$  while for the incubation

with the spike protein the increase was  $40 \pm 9\%$ . The signal/noise factor (S/N) was calculated as the ratio between  $\Delta R_{ct}$  obtained for the target protein (S) and the  $\Delta R_{ct}$  obtained for the protein used as the negative control (N). Thus, the S/N factor calculated for the NS1ZV was 2.4 and for the spike was 3.4, which demonstrates the selectivity of this biosensor.

For the Zika biosensor, the cross-reactivity test was performed with NS1DV and spike proteins. The  $\Delta R_{ct}$  values obtained were  $55 \pm 5\%$  for NS1DV and  $63 \pm 2\%$  for spike. The comparative analysis of the biosensor response for the different samples is shown in Fig. 4b. It is observed that the Zika biosensor was even more selective, presenting an S/N factor of 4.6 for NS1DV and 4 for the spike. These results show that the surface modification procedure was effective for target protein biorecognition for the two biosensors. In addition, they showed

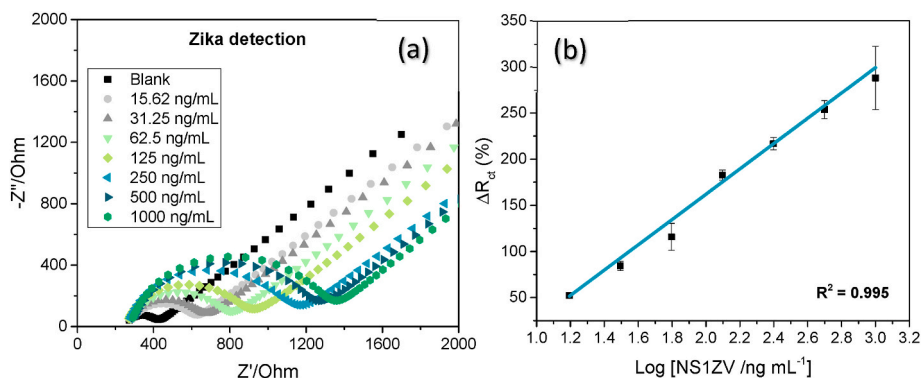


**Fig. 6.** Analytical curve of the Zika biosensor in the range of 15.62–1000 ng/mL. The Nyquist plots (a) and the analytical curve (b) show a linear relationship between the percent change in  $R_{ct}$  and the logarithm of the concentration of NS1ZV. Each concentration was tested on 3 independent electrodes ( $n = 3$ ).

**Table 1**

Tests for simultaneous detection of Zika and Dengue reported in the literature.

Analytical technique	Analyte	LOD Zika (detection range)	LOD Dengue (detection range)	Ref.
Fluorescence	RNA	184 pM (0.5–70 nM)	121 pM (1–60 nM)	Xie et al. (2018)
Fluorescence	RNA	5.2 nM (10–40 nM)	2.1–5.9 nM (10–40 nM)	Lee et al. (2020)
RT-PCR	RNA	10 <sup>3</sup> GCE/mL (10 (Sarkar and Gardner, 2016)-10 (Faria and Zucolotto, 2019) GCE/mL)	10 <sup>3</sup> GCE/mL (10 (Sarkar and Gardner, 2016)-10 (Faria and Zucolotto, 2019) GCE/mL)	Santiago et al. (2018)
Magnetic relaxation	antibodies	10 ng/mL (10–120 nM)	Not mentioned (10–120 nM)	Banerjee et al. (2021)
Surface-enhanced Raman spectroscopy	NS1 proteins	0.72 ng/mL (10–500 ng/mL)	7.67 ng/mL (10–500 ng/mL)	Sánchez-Purrà et al. (2017)

excellent selectivity when analyzed with biomarker proteins from other viral diseases that, in early stages, cause similar symptoms.

### 3.3. Analytical curves and biosensor performance

To provide a quantitative diagnosis, the impedance response for different analyte concentrations was evaluated for each biosensor and analytical curves were obtained. For the Dengue biosensor, the Nyquist diagram (Fig. 5a) shows that the  $R_{ct}$  gradually increases with the concentration of NS1DV. The analytical curve (Fig. 5b) exhibited a linear relationship between the  $\Delta R_{ct}$  and the logarithm of the NS1DV concentration in the range of 15.62–500.00 ng/mL. The equation determined from the linear regression was  $\Delta R_{ct} (\%) = -47.85 + 68.50 \times \log_{10}(\text{NS1DV concentration}/\text{ng mL}^{-1})$ , with a correlation coefficient ( $R^2$ ) of 0.990. According to the IUPAC model, the limit of detection (LOD), which indicates the lowest concentration of analyte that the device can detect, was 1.17 ng/mL.

The Zika biosensor also presented an impedance variation as a function of the analyte concentration (Fig. 6a). A linear relationship between the  $\Delta R_{ct}$  and the logarithm of the NS1ZV concentration was obtained from 15.62 ng/mL to 1000.00 ng/mL (Fig. 6b). The equation best fitted was  $\Delta R_{ct} (\%) = -112.09 + 137.07 \times \log_{10}(\text{NS1ZV concentration}/\text{ng mL}^{-1})$ , with  $R^2$  of 0.995. The standard deviation of blank measurements and the LOD obtained were 24.7% and 0.54 ng/mL, respectively. For both biosensors, LOD values are much lower than the typical plasma NS1 concentrations in the first days of infection, indicating that the multiplex device is a good alternative for the early diagnosis of Zika and Dengue.

To assess the performance of the developed biosensors, reproducibility and repeatability tests were carried out, which are important parameters, especially for disposable devices aimed at point-of-care applications. These tests were performed only for the Zika biosensor since both biosensors were fabricated on the same platform (multiplex device) and with the same methodology. Tests were performed after incubation for 30 min with a negative sample, containing spike proteins at 0.5  $\mu\text{g/mL}$ . The relative standard deviation (RSD) for the three consecutive measurements on the same electrode was 11.7%, as shown in Fig. S2 (Supporting Information). The reproducibility was determined from the percent change of  $R_{ct}$  for four different electrodes (Fig. S3, Supporting Information), an RSD of 9.7% was obtained. These results show that the developed biosensors have excellent reproducibility (RSD <10%) and good repeatability (RSD close to 10%) and, therefore, follow the criteria established by the Clinical and Laboratory Standards Institute (CLSI; EP06) for quantitative tests based on an analytical curve. Compared to other biosensors for simultaneous detection of Zika and Dengue (see Table 1), our device features a simple sample preparation and analysis technique, facilitating its point-of-care application. The conventional ELISA test, which is the gold standard diagnostic method for these diseases, requires trained users and takes about 6 h (Hu et al., 2020) and using the commercial kits for detection of NS1 proteins, the estimated price per test is about US\$ 11 for Dengue (MBS3801930, Mybiosource, USA) and US\$ 4 for Zika (MBS8123983, Mybiosource, USA), totaling US\$ 15. Our chip for simultaneous detection of Zika and Dengue costs about US\$ 4 and takes 10 min to provide the result. Therefore, it represents a diagnostic platform both easy-to-use and

cost-effective.

## 4. Conclusion

A multiplex device for electrochemical detection of Zika and Dengue viruses on a single chip was developed. The dengue biosensor presented a linear relationship between  $\Delta R_{ct}$  and the logarithm of the NS1DV concentration for the range 15.62–500.00 ng/mL and the LOD obtained was 1.17 ng/mL. For the Zika biosensor, the linear relationship of the  $\Delta R_{ct}$  with the logarithm of the NS1ZV concentration was observed for the range 15.62–1000.00 ng/mL, and a LOD of 0.54 ng/mL was achieved. The biosensors showed good reproducibility (RSD of 9.7%) and repeatability (RSD of 11.7%). More importantly, no cross-reactivity was observed for NS1DV, NS1ZV, and spike proteins tested in both biosensors, demonstrating their excellent selectivity. Therefore, this device can be used in the differential diagnosis of Zika and Dengue at early stages, offering a unique test for the rapid and point-of-care detection of these diseases. In addition, due to the device design, which includes four working electrodes, it is possible to add biosensors for two other diseases, which is very advantageous for regions where diseases with similar symptoms are endemic.

### CRedit authorship contribution statement

**Isabella Sampaio:** Conceptualization, Methodology, Formal analysis, Writing – original draft, Writing – review & editing. **Felipe Domingues Quatroni:** Methodology, Formal analysis, Writing – review & editing. **Juliana Naomi Yamauti Costa:** Methodology, Formal analysis, Writing – review & editing. **Valtencir Zucolotto:** Writing – review & editing, Funding acquisition, Supervision.

### Declaration of competing interest

The authors declare that they have no known competing financial interests or personal relationships that could have appeared to influence the work reported in this paper.

### Data availability

The data that has been used is confidential.

### Acknowledgments

We gratefully acknowledge to the National Council for Scientific and Technological Development - CNPq (Grant numbers 440496/2016-0, 381473/2019-8 and 88887.514070/2020), Higher Education Personnel Improvement Coordination – CAPES (Grant number 88881.130763/2016-01) and São Paulo Research Foundation - FAPESP (Grant number 2019/21497-7) for the financial support and the researchers from Nanomedicine and Nanotoxicology Group for their cooperation in our studies.

### Appendix A. Supplementary data

Supplementary data to this article can be found online at <https://doi.org/10.1016/j.bios.2022.114630>.

org/10.1016/j.bios.2022.114630.

## References

- Bachour Junior, B., Batistuti, M.R., Pereira, A.S., de Sousa Russo, E.M., Mulato, M., 2021. Electrochemical aptasensor for NS1 detection: towards a fast dengue biosensor. *Talanta* 233, 122527.
- Banerjee, T., Patel, T., Pashchenko, O., Elliott, R., Santra, S., 2021. Rapid detection and one-step differentiation of cross-reactivity between zika and dengue virus using functional magnetic nanosensors. *ACS Appl. Bio Mater.* 4, 3786–3795.
- Bosch, I., et al., 2017. Rapid antigen tests for dengue virus serotypes and zika virus in patient serum. *Sci. Transl. Med.* 9, 1–14.
- Brito, A.F., et al., 2021. Lying in wait: the resurgence of dengue virus after the Zika epidemic in Brazil. *Nat. Commun.* 12, 1–13.
- Butterworth, A., et al., 2019. SAM composition and electrode roughness affect performance of a DNA biosensor for antibiotic resistance. *Biosensors* 9.
- Cecchetto, J., Santos, A., Mondini, A., Cilli, E.M., Bueno, P.R., 2020. Serological point-of-care and label-free capacitive diagnosis of dengue virus infection. *Biosens. Bioelectron.* 151, 111972.
- Dias, A.C.M.S., Gomes-Filho, S.L.R., Silva, M.M.S., Dutra, R.F., 2013. A sensor tip based on carbon nanotube-ink printed electrode for the dengue virus NS1 protein. *Biosens. Bioelectron.* 44, 216–221.
- Dutta, G., Fernandes, F.C.B., Estrela, P., Moschou, D., Bueno, P.R., 2021. Impact of surface roughness on the self-assembling of molecular films onto gold electrodes for label-free biosensing applications. *Electrochim. Acta* 378, 138137.
- Faria, H.A.M., Zucolotto, V., 2019. Label-free electrochemical DNA biosensor for zika virus identification. *Biosens. Bioelectron.* 131, 149–155.
- Hu, R., Sou, K., Takeoka, S., 2020. A rapid and highly sensitive biomarker detection platform based on a temperature-responsive liposome-linked immunosorbent assay. *Sci. Rep.* 10, 1–11.
- Lee, J.S., Kim, J., Shin, H., Min, D.H., 2020. Graphene oxide-based molecular diagnostic biosensor for simultaneous detection of Zika and dengue viruses. *2D Mater.* 7.
- Lima, M., da, R.Q., et al., 2019. The inability of a dengue NS1 ELISA to detect Zika infections. *Sci. Rep.* 9, 1–7.
- Priye, A., et al., 2017. A smartphone-based diagnostic platform for rapid detection of Zika, chikungunya, and dengue viruses. *Sci. Rep.* 7, 1–11.
- Rajah, M.M., Pardy, R.D., Condotta, S.A., Richer, M.J., Sagan, S.M., 2016. Zika virus: emergence, phylogenetics, challenges, and opportunities. *ACS Infect. Dis.* 2, 763–772.
- Sánchez-Purrà, M., et al., 2017. Surface-enhanced Raman spectroscopy-based sandwich immunoassays for multiplexed detection of zika and dengue viral biomarkers. *ACS Infect. Dis.* 3, 767–776.
- Santiago, G.A., et al., 2018. Performance of the Trioplex real-time RT-PCR assay for detection of Zika, dengue, and chikungunya viruses. *Nat. Commun.* 9.
- Santos, A., Bueno, P.R., Davis, J.J., 2018. A dual marker label free electrochemical assay for Flavivirus dengue diagnosis. *Biosens. Bioelectron.* 100, 519–525.
- Sarkar, S., Gardner, L. Zika, 2016. The cost of neglect. *Palgrave Commun* 2, 1–6.
- WHO. Dengue and Severe Dengue, 2021. WHO Fact Sheet.
- Wilder-Smith, A., Ooi, E.E., Horstick, O., Wills, B., 2019. Dengue. *Lancet* 393, 350–363.
- Xie, B.P., et al., 2018. Simultaneous detection of Dengue and Zika virus RNA sequences with a three-dimensional Cu-based zwitterionic metal-organic framework, comparison of single and synchronous fluorescence analysis. *Sensor. Actuator. B Chem.* 254, 1133–1140.
- Yang, K.H., Narayan, R.J., 2017. Analytical methods for detection of Zika virus. *MRS Commun* 7, 121–130.